ISLETS
2019, VOL. 11, NO. 2, 21–32
https://doi.org/10.1080/19382014.2019.1581544

Taylor & Francis
Taylor & Francis Group

RESEARCH PAPER

OPEN ACCESS Check for updates

# Gene expression patterns in synchronized islet populations

Nikita Mukhitov *, Joel E. Adablah, and Michael G. Roper

Department of Chemistry and Biochemistry, Florida State University, Tallahassee, FL

**ABSTRACT**

In vivo levels of insulin are oscillatory with a period of ~5–10 minutes, indicating that the islets of Langerhans within the pancreas are synchronized. While the synchronizing factors are still under investigation, one result of this behavior is expected to be coordinated and oscillatory intracellular factors, such as intracellular $Ca^{2+}$ levels, throughout the islet population. In other cell types, oscillatory intracellular signals, like intracellular $Ca^{2+}$, have been shown to affect specific gene expression. To test how the gene expression landscape may differ between a synchronized islet population with its reproducible intracellular oscillations and an unsynchronized islet population with heterogeneous oscillations, gene set enrichment analysis (GSEA) was used to compare an islet population that had been synchronized using a glucose wave with a 5-min period, and an unsynchronized islet population. In the population exposed to the glucose wave, 58/62 islets showed synchronization as evidenced by coordinated intracellular $Ca^{2+}$ oscillations with an average oscillation period of 5.1 min, while in the unsynchronized population 29/62 islets showed slow oscillations with an average period of 5.2 min. The synchronized islets also had a significantly smaller drift of their oscillation period during the experiment as compared to the unsynchronized population. GSEA indicated that the synchronized population had reduced expression of gene sets related to protein translation, protein turnover, energy expenditure, and insulin synthesis, while those that were related to maintenance of cell morphology were increased.

**ARTICLE HISTORY**
Received 16 August 2018
Revised 14 January 2019
Accepted 31 January 2019

**KEYWORDS**
Islet of Langerhans; synchronization; glucose; gene expression; microfluidic

## Introduction

Pancreatic islets are key modulators of glucose homeostasis through the release of insulin and other hormones.[1] Secretion of these hormones is dynamic occurring in an oscillatory secretion rhythm that encompasses timescales from minutes to hours. While circadian[2] and ultradian[3] insulin oscillations are responsible for the longer timescale dynamics, the rapid pulses observed *in vivo* with periods ranging from 5- to 10-min[4-7] are less characterized. Notably, it has been shown that diminished insulin oscillations are one of the first observable features of type 2 diabetes.[8]

One long standing hypothesis of how the numerous islets in the pancreas synchronize to produce the in vivo oscillations is through classic insulin-glucose feedback loops, which would result in oscillatory glucose and insulin levels, both of which have been observed.[9-12] This hypothesis has been tested using a microfluidic system where glucose was delivered to a population of islets with the levels iteratively adjusted by a mathematical model that mimicked insulin-dependent glucose uptake.[12] With the appropriate parameters of the model, the islets synchronized resulting in population level oscillations of insulin secretion and glucose levels. The average period to which the system converged was ~5 min, similar to the period of insulin secretion observed *in vivo*.

In this manuscript, we explore if a synchronized islet population has a different gene expression compared to an unsynchronized islet population. The reason for this exploration is that a synchronized islet population has been shown to not only produce a coherent insulin output, but also synchronized intracellular metabolites, including, some that have been shown in other cellular systems to affect gene expression levels, for example, $Ca^{2+}$ oscillations.[13-16] Synchronization would be expected to not only force some islets to oscillate at a different frequency than their natural frequency, but it would also produce a more consistent oscillation period in these

**CONTACT** Michael G. Roper roper@chem.fsu.edu Department of Chemistry and Biochemistry, Florida State University, 95 Chieftain Way, Tallahassee, FL, 32306.
*Nikita Mukhitov is currently affiliated with the Department of Biological Engineering, Massachusetts Institute of Technology, Cambridge, MA.
Supplemental data for this article can be accessed on the publisher's website.

© 2019 The Author(s). Published with license by Taylor & Francis Group, LLC.
This is an Open Access article distributed under the terms of the Creative Commons Attribution-NonCommercial-NoDerivatives License (http://creativecommons.org/licenses/by-nc-nd/4.0/), which permits non-commercial re-use, distribution, and reproduction in any medium, provided the original work is properly cited, and is not altered, transformed, or built upon in any way.

intracellular signals than a non-synchronized population due to the driving rhythm. We expect that this consistent and unique oscillation frequency in the synchronized population would result in different gene expression patterns than islets in the non-synchronized population which would experience more irregular dynamics. Changes in gene expression could shed light on the effects and possible benefits of islet synchronization at the cellular level.

To investigate the effect of synchronization on islet gene expression, an islet population was synchronized by delivering a 5-min period, 11 ± 1 mM glucose wave,[17,18] lysed, and gene expression levels measured using microarray analysis. A control group of islets were similarly exposed to 11 mM glucose, but without a wave, lysed, and levels measured using a microarray. Gene set enrichment analysis[19,20] (GSEA) was performed to evaluate gene expression patterns and states. The results indicated that the synchronized population had reduced expression of gene sets related to protein translation, protein turnover, energy expenditure, and insulin synthesis, while those that were related to maintenance of cell morphology were increased.

## Materials and methods

### Chemical reagents and supplies

Cosmic calf serum, dimethyl sulfoxide (DMSO), fluorescein, 4-(2-hydroxyethyl)-1-piperazineethanesulfonic acid (HEPES), $MgCl_2$, NaCl, pluronic F-127, RPMI 1640, and an antibiotic/antimycotic solution were obtained from Sigma-Aldrich (St. Louis, MO). Dextrose was obtained from Fisher Scientific (Pittsburgh, PA). $CaCl_2$, KCl, and NaOH were obtained from EMD Chemicals (Gibbstown, NJ). Fura-2 acetoxymethyl ester (Fura-2 AM) was obtained from Invitrogen (Carlsbad, CA). Poly(dimethyl siloxane) (PDMS) elastomer kit was obtained from Dow Corning (Midland, MI).

For all islet stimulation experiments, a balanced salt solution (BSS) was used. BSS was composed of 125 mM NaCl, 2.4 mM $CaCl_2$, 1.2 mM $MgCl_2$, 5.9 mM KCl, 25 mM HEPES, and adjusted to pH 7.4. The BSS was further supplemented with either 3 or 13 mM glucose. Fura 2-AM stock was prepared by reconstitution in 10 μL of pluronic F127 and 10 μL of DMSO. The prepared stock was stored protected from light at room temperature.

### Isolation and handling of islets of Langerhans

All experiments were performed under guidelines approved by the Florida State University Animal Care and Use Committee (ACUC) protocol #1519. Islets were isolated from 20–40 g male CD-1 mice (Charles River Laboratories, Wilmington, MA) as previously described.[20,21] Briefly, mice were euthanized by $CO_2$ inhalation. The pancreas was then inflated by injection of 5 mL of collagenase through the common bile duct. The inflated pancreas was excised and incubated in 5 mL of collagenase solution at 37°C for 10 min. Islets were picked by hand under a stereomicroscope. Islets were selected that had a spherical shape, a smooth surface, indicative of an intact islet membrane, and a diameter of 50–150 μm. The islets were placed in RPMI 1640 cell culture media supplemented with 10% cosmic calf serum, and incubated at 37°C, 5% $CO_2$. For each set of experiments, islets were isolated from at least three mice and equally pooled from each animal (e.g., 40 islets were taken from three mice to a total of 120). From this pooled collection, islets were randomly selected for stimulation and $Ca^{2+}$ imaging. All experiments were conducted within two days of isolation.

### Experimental setup

Microfluidic devices were made from PDMS and fabricated using conventional soft lithography.[21] The design used in this study was described in previous work.[12] Imaging of $Ca^{2+}$ was performed as previously described.[12] Briefly, the microfluidic device was positioned on the stage of a Nikon Ti-S microscope equipped with a 10X, 0.5 NA objective (Nikon Instruments, Melville, NY). Excitation was achieved with a Xenon arc lamp equipped with an integrated shutter and filter wheel (Sutter Instruments, Novato, CA). Acquisition was performed on a charge coupled device (CCD) camera (Photometrics, Tucson, AZ). Nikon NIS Elements software was used to control the camera, shutter, and filter wheel. During imaging, excitation was performed sequentially at 340 ± 5.5 and 380 ± 5.5 nm (Chroma, Bellows Falls, VT).

Emission was filtered through a 415 nm long pass dichroic mirror and a 510 ± 20 nm emission filter (Omega, Brattleboro, VT). The response of islets is given as a ratio of fluorescence emission generated from excitation at 340 and 380 nm (F340/F380). Imaging was performed every 30-s with 100-ms exposure per excitation channel.

### Islet stimulation and imaging

Fura 2-AM was loaded into islets in serum free RPMI 1640 medium for 42 min in an incubator controlled at 37°C and 5% $CO_2$. After loading with dye, 6 or 7 islets were placed in the microfluidic device and perfused with BSS containing 3 mM glucose for 1-min to wash them free of media. The experiment then commenced by perfusing islets with BSS containing 3 mM glucose for 2-min. After 2-min, the glucose challenge was applied in either a constant manner at 11 mM or as a sinusoidal wave with a median value of 11 mM, an amplitude of 1 mM, and a 5-min period. The stimulation was maintained for 80-min.

Following the 82-min experiment, the islets were extracted and lysed using the Qiagen RNeasy plus micro kit (Qiagen, Hilden, Germany). The lysate was homogenized and held at room temperature for 10-min. The lysate was then flash frozen in liquid $N_2$ and held at −80°C. Once all islet experiments were completed and the lysates frozen, the samples were thawed and the total RNA from each sample was purified using spin columns from the RNeasy plus micro kit. Purified total RNA was reconstituted in RNAse-free water. Approximate RNA yields were 15 ng/islet and RIN values of 10.0 were observed for all samples analyzed. Each glucose stimulation protocol was performed two more times and the total RNA from 21 islets were pooled and analyzed on a single microarray. Islets from different mice were then stimulated using one of the two glucose protocols, lysed, and pooled in the same manner for biological replicates on additional microarrays. Three Affymetrix Mouse Gene 2.0 ST microarrays were used for each glucose experimental protocol.

### Data analysis

Mouse Gene 2.0 ST CEL files were normalized to produce gene-level expression values using the implementation of the Robust Multiarray Average (RMA)[22] in the affy package (version 1.36.1)[23] included in the Bioconductor software suite (version 2.12)[24] and an Entrez Gene-specific probeset mapping (17.0.0) from the Molecular and Behavioral Neuroscience Institute (Brainarray) at the University of Michigan.[25,] Array quality was assessed by computing Relative Log Expression (RLE) and Normalized Unscaled Standard Error (NUSE) using the affyPLM package (version 1.34.0).[26] Principal Component Analysis (PCA) was performed using the prcomp R function with expression values that had been normalized across all samples to a mean of zero and a standard deviation of one. Differential expression was assessed using the moderated (empirical Bayesian) t-test implemented in the limma package (version 3.14.4). Correction for multiple hypothesis testing was accomplished using the Benjamini-Hochberg false discovery rate (FDR).[27] Human homologs of mouse genes were identified using HomoloGene (version 68).[28] All microarray analyses were performed using the R environment for statistical computing (version 2.15.1).

GSEA (version 2.2.1)[19] was used to identify biological terms, pathways and processes that were coordinately up- or down-regulated within each pairwise comparison. The Entrez Gene identifiers of the human homologs of the genes interrogated by the array were ranked according to the moderated t-statistic computed between the two experimental conditions. Mouse genes with multiple human homologs (or vice versa) were removed prior to ranking. The ranked list represented only those human genes that matched exactly one mouse gene. This ranked list was then used to perform pre-ranked GSEA analyses (default parameters with random seed 1234) using the Entrez Gene versions of the Hallmark, Biocarta, KEGG, Reactome, Gene Ontology (GO), and transcription factor and microRNA motif gene sets obtained from the Molecular Signatures Database (MSigDB), version 5.0.[20]

The overlap between the different nodes was visualized by the generation of an enrichment map using the results from the GSEA analysis which were input into the Cytoscape software suite (version 3.5.1).[29] The map was constructed

with a cutoff of $p < 0.05$ and an FDR cutoff of $q < 0.25$. The similarity cutoff was 0.5 with a combined constant of 0.5. The MCL cluster algorithm was used to group the nodes into clusters.

For determination of $Ca^{2+}$ drift, Fura-2 traces were analyzed in GraphPad Prism 7 software (La Jolla, CA) that allowed for interpolation of data points. The first peak after a stimulus was disregarded. The beginning of an oscillation period was determined as the time point prior to the start of a peak rise ($t_{start}$). The period (p) was defined as the difference in time between two adjacent start times ($p = t_{start+1} - t_{start}$). The periods were then plotted as a function of elapsed experimental time and a linear regression was fit to the data. The absolute value of the slope of the linear regression (Δp/time) to this plot was defined as the drift. For testing statistical significance, unless otherwise stated, a paired, two-tailed t-test was employed. All data used to generate the figures are provided in a supplementary file.

## Results

We expected that islets which were entrained to a common forcing signal (a glucose wave with a 5 min period) would have highly synchronized and regular oscillations of intracellular signals compared to unforced, and therefore unsynchronized, groups of islets. These differences in oscillation patterns may then produce differences in gene expression profiles. In the experiments described below, the difference in the synchronized populations, as determined by the $Ca^{2+}$ oscillations between synchronized and unsynchronized groups of islets, were quantified, and the gene expression profiles, as determined by microarrays, were evaluated using GSEA.

### *Characterization of $Ca^{2+}$ dynamics*

We first set out to quantify the difference in $Ca^{2+}$ oscillation dynamics between synchronized and unsynchronized populations. While other intracellular signals could be responsible for differences in the gene expression profiles between the islet populations, we examined the intracellular $Ca^{2+}$ levels for two reasons: $Ca^{2+}$ oscillation frequency has been shown to affect gene expression in other cell types,[13-16] and intracellular $Ca^{2+}$ has been shown to be coordinated with other intracellular factors (some examples include NAD(P)H, and mitochondrial membrane potential[10]). As a result, imaging of intracellular $Ca^{2+}$ serves a probe for multiple intracellular dynamics.

As shown in Figure 1(a), when a population of islets were exposed to 11 ± 1 mM glucose wave with a 5-min period, the $Ca^{2+}$ oscillations from 93.5% of the islets (58/62) entrained to the glucose wave, exhibiting a period of 5.1 min (Table 1). This entrainment persisted throughout the duration of the experiment resulting in a highly homogenous population as seen in the heatmap of Figure 1(a).

For the group of islets that were exposed to a constant glucose concentration, only 46.8% showed oscillations close to 5-min (average period of 5.2 min), yet they were not synchronized, as can be seen in the heatmap in Figure 1(b). Representative examples of the numerous other types of $Ca^{2+}$ dynamics that were observed in this group are shown in Figure S1 with all oscillation types summarized in Table 1. All of these various oscillation modes are similar to those that have been reported elsewhere.[30,31] Disregarding the heterogeneous $Ca^{2+}$ dynamics in this group, there was still a difference in the slow oscillation dynamics between the two islet populations. This can be seen by the difference in the standard deviations of the two population oscillation periods, with a lower standard deviation in the synchronized islets (0.7 min) as compared to the non-synchronized population (1.2 min) (Table 1).

Overall, these data re-confirmed previous findings[7,10,12,17,18,32] that islets exposed to a 5-min glucose wave are entrained and have high homogeneity in their $Ca^{2+}$ response, whereas islets exposed to a constant glucose dose are oscillatory, but the individual responses vary widely. It should be noted that under the oscillatory glucose delivery, the $Ca^{2+}$ oscillations from the groups of islets are not only synchronized, but so is the insulin release. Using a fluorescence anisotropy immunoassay[33], a group of 7 islets synchronized their insulin release upon exposure to a 5-min period glucose wave (Figure S2). The synchronization is observed as coherent pulses of insulin from the group and is similar to what we have demonstrated in previous experiments.[7,12]

Importantly, the islets exposed to a constant glucose level did not only have large heterogeneity in oscillation dynamics, we also observed that individual islets within that population did not maintain

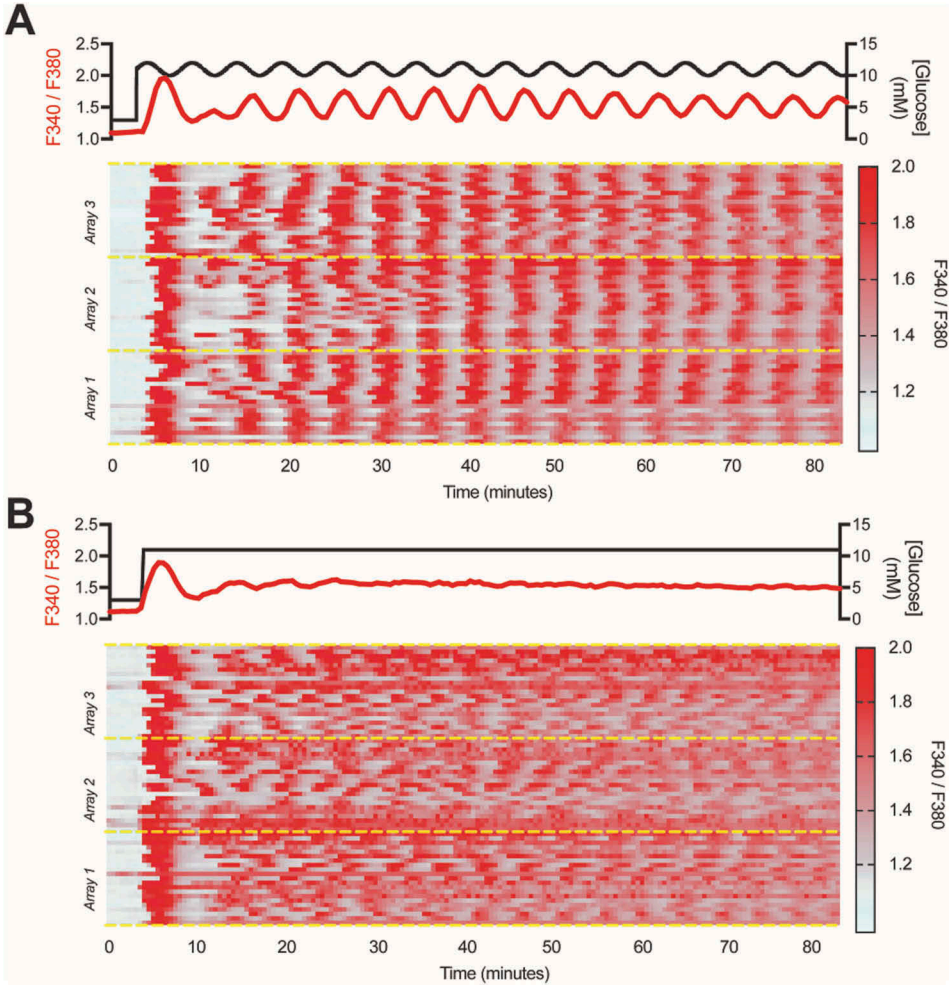


**Figure 1.** Effect of glucose profiles on islet response. The administered glucose dose (black trace) is plotted on top of each panel. The average F340/F380 signal from all islets in each glucose protocol is plotted at the top of the panels in red. The individual islet signatures are shown in a heatmap. The groupings for the microarrays are delineated with yellow dotted lines. (a) When exposed to 11 ± 1 mM glucose wave with a 5-min period, the islets synchronized as seen by the homogeneous F340/F380 ratio across the population. (b) When exposed to a constant 11 mM glucose, the islets oscillated at unique periods with different phases to one another, resulting in an incoherent population.

**Table 1.** Distribution of oscillation types.

| Type | Constant | Wave |
|---|---|---|
| Slow Oscillator (%) | 46.8 | 93.5 |
| *Avg (min)* | *5.2* | *5.1* |
| *SD (min)* | *1.2* | *0.7* |
| Compound Oscillator (%) | 24 | 3 |
| Fast Oscillator (%) | 15 | 0 |
| Stopped Oscillating (%) | 11 | 3 |
| Not Oscillating (%) | 3 | 0 |

a constant oscillation period throughout the experiment. To showcase this "drift", the periods of the $Ca^{2+}$ oscillations from two representative islets given the two glucose treatments are shown overlapped with their Fura-2 traces (Figure 2(a,b)). When exposed to a glucose wave, the islet in Figure 2(a) entrained to the driving frequency and maintained a constant period. In contrast, when exposed to a constant glucose level, the islet in Figure 2(b) also showed slow oscillations, but the period of its oscillations varied from 8.6 to 4.5 min. The presence of drift was inspected in all islets showing "slow" oscillations exposed to the wave (n = 58/62) and constant (n = 29/62) glucose treatments. The average drift was significantly lower for islets exposed to the glucose wave (0.12 ± 0.01 minutes/minute) compared to those exposed to the constant glucose level (0.23 ± 0.02 minutes/minute) ($p = 0.001$) (Figure 2(c)).

In summary, the delivery of an oscillatory glucose level produced the expected entrainment with homogeneous oscillations from the islet population. These coherent oscillations had tight distributions of

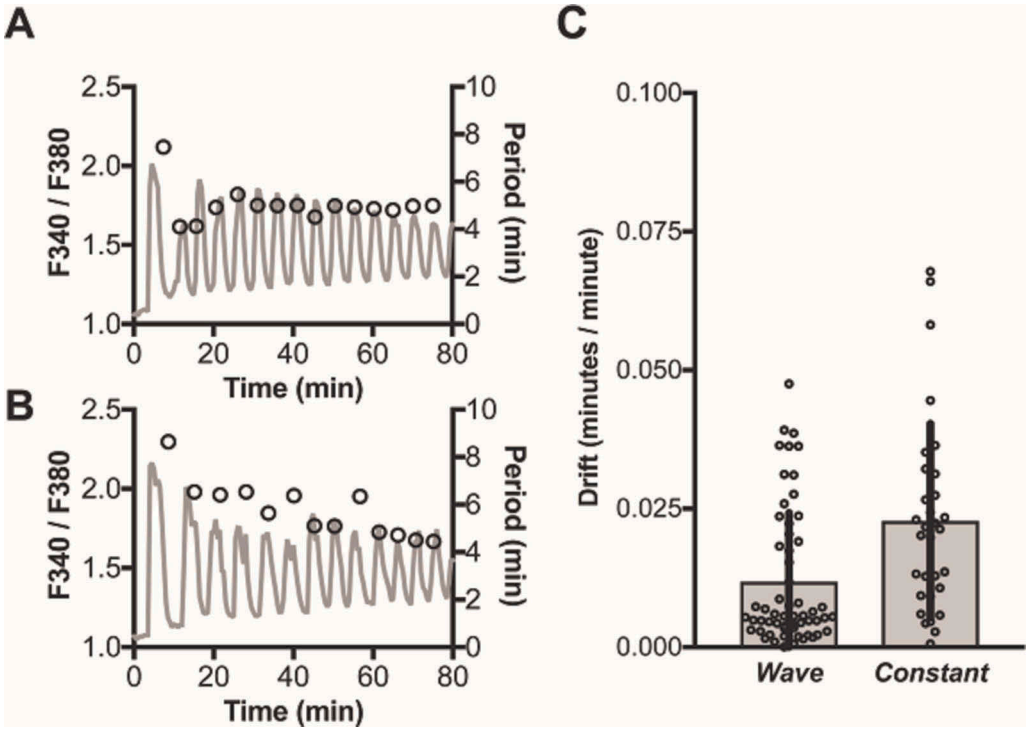


**Figure 2.** Analysis of islet calcium signatures. Representative single islet $Ca^{2+}$ level (gray lines) from an islet exposed to 11 ± 1 mM glucose wave with a 5-min period (a) and a constant 11 mM glucose level (b). The black hollow circles (o) above the traces are the measured period for each oscillation and corresponds to the right y-axis. (c). The average drift, calculated as described in the text, from islets showing a "slow" oscillation mode is given by the gray bars with the error bars corresponding to ± 1 SD. Individual values of the drift are plotted as black hollow circles (o).

the oscillation period with little drift. Conversely, islets exposed to a constant glucose level were not synchronized and produced a wide range and large drift of oscillation periods. Considering this data, and with the precedent of oscillation frequency affecting gene expression,[13-16] we continued the investigation to determine if differences in gene expressions between the populations were observed.

### *Differential expression of genes in synchronized islet populations*

To examine gene expression levels, microarray analysis was used to measure mRNA from islets exposed to the two glucose stimulation protocols. Initial tests on the array results were performed by principal component analysis (Figure S3A). The first component accounted for 25% of the variability and demonstrated well-defined separation. Clustering along the second component was low, but we attribute this to both islet populations having similar responses to the same dose of glucose (oscillations with a period of ~5 min). The larger proportion of low p-values compared to high p-values (Figure S3B) confirmed differential expression of genes between synchronized and non-synchronized islet populations. 400 genes were differentially expressed with p-values < 0.01 and over 2,000 with p-value < 0.05 (Figure S3C). Considering that the glucose dose was the same for both sets of islets and that both sets induced oscillations, the finding of only a small set of differentially expressed genes between the two treatments is not surprising.

To analyze these data, GSEA was used to compare the differentially regulated groups of genes between the two islet populations. Rather than evaluating the expression at the single gene level, GSEA examines gene sets corresponding to particular pathways that were curated and compiled *a priori*. This grouping lowers the rate of false positives and increases the statistical robustness of the experiment.[19] This type of analysis has been shown to be useful in identifying gene sets associated with diabetic retinopathy,[34,35] mature onset diabetes of the young,[35] type I and II diabetes,[19] and cancer subtypes[36] amongst others.

Several gene sets were found to be statistically enriched in synchronized islets and a selection is

summarized in Figure 3. The gene sets were filtered to normalized enrichment scores (NES) > 1.7 and FDRq < 0.25, which produced 59 sets that were up-regulated and 286 that were down-regulated in islets that were synchronized. The three largest gene set clusters were "G1 Organization", "Biosynthesis", and "Membrane, ER and Respiration" with 44, 38 and 30 clustered gene sets, respectively (please see the enrichment map in Figure 4). Several clusters from KEGG pathways were found to be differentially regulated, including up-regulated ECM-receptor interactions (NES = 1.870) and cytokine-cytokine receptor interactions (NES = 1.842), while N-glycan biosynthesis (NES = −2.335) and protein export (NES = −2.397) were down-regulated. These findings agreed with several of the Reactome gene sets. Specifically, the set for tight-junction interaction (NES = 1.840) was up-regulated, and asparagine N-linked glycosylation (NES = −2.536) was strongly down-regulated. Other Reactome sets of interest were unfolded protein response (NES = −2.146) and Diabetes pathway (NES = −2.146), both down-regulated. The GO groupings also demonstrated similar patterns as the other curated gene set databases. The GO terms revealed a down-regulation of cellular respiration (NES = −1.797) and protein amino acid n-linked glycosylation (NES = −1.967), and an up-regulation of cell membrane terms, e.g. extracellular matrix (NES = 1.676). Several terms associated with biosynthesis and catabolism were

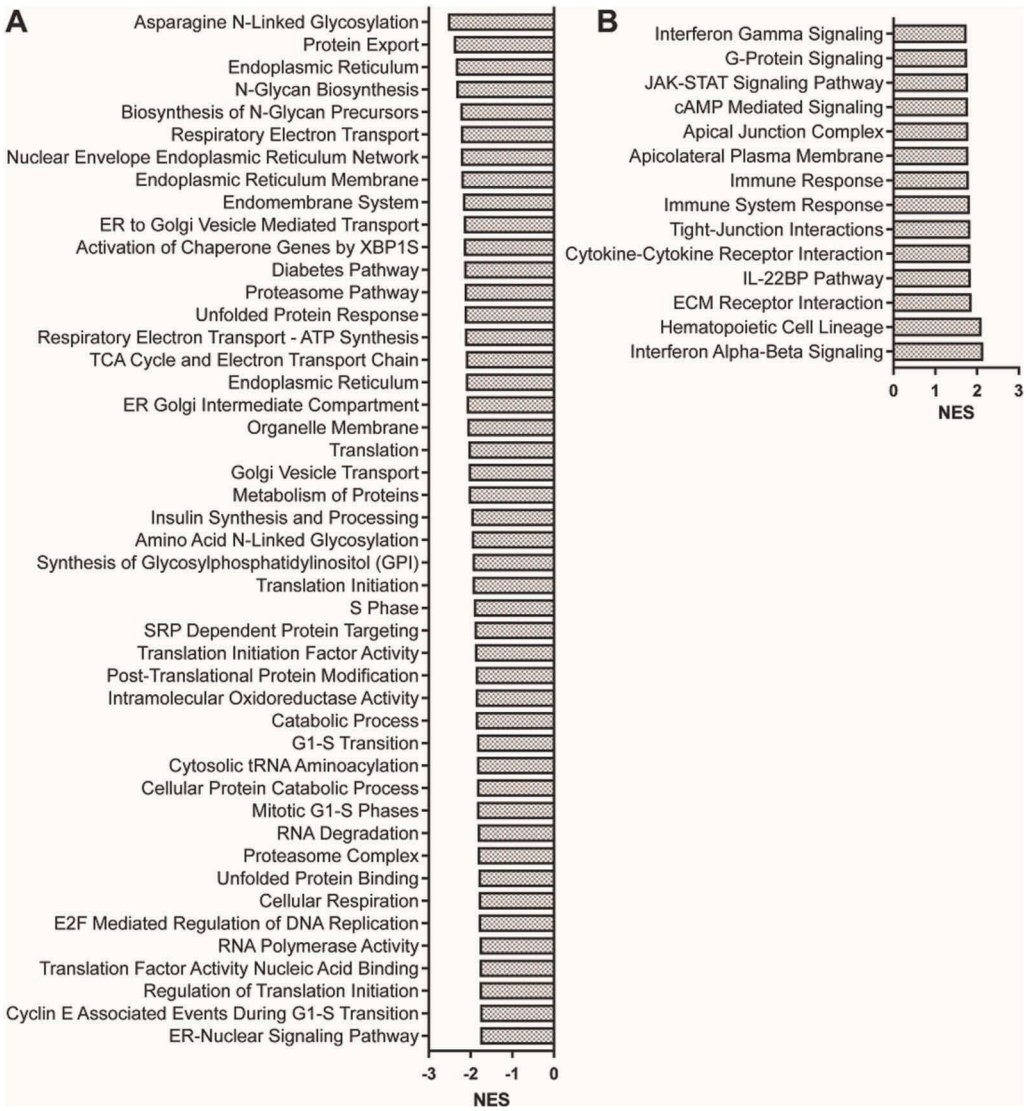


**Figure 3.** Overview of GSEA results. Gene sets down-regulated (a) and up-regulated (b) in synchronized islets. Only a set of selected sets with NES > 1.75 are shown, with the full list available in the Supplementary Information.

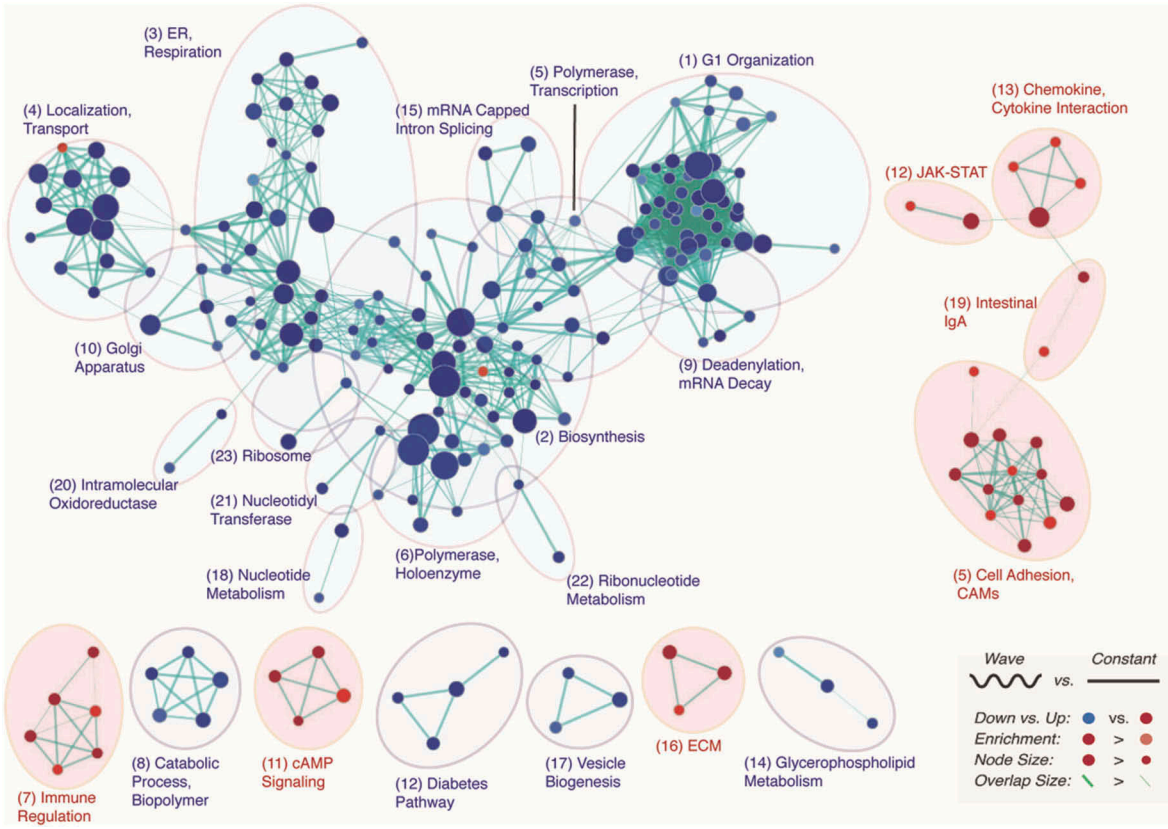


**Figure 4.** Enrichment map. The enrichment map enables visualization of the general gene expression landscape of the synchronized population compared to the unsynchronized population. The key is shown in the bottom right of the figure. Each node corresponds to a gene set from the GSEA data, and the thickness of the lines connecting the nodes is proportional to the number of genes that overlap in the gene set. Those sets that are up-regulated in the wave treatment are shown in red and those down-regulated are shown in blue. Clustering among the various gene sets is visualized with circles over the nodes. The clusters are ranked by the number of common nodes and the rank is shown in parentheses.

downregulated in entrained islets. Specifically, protein catabolic processes (NES = −1.841), proteasome complex (NES = −1.831), metabolism of proteins (NES = −2.043), translation (NES = −2.050) and insulin synthesis and processing (NES = −1.979) gene sets were downregulated. Other down-regulated metabolism associated sets included TCA cycle and respiratory electron transport (NES = −2.108) and respiratory electron transport (NES = −2.226). Finally, several terms associated with the endoplasmic reticulum were also found to be down-regulated: ER to Golgi vesicle mediated transport (NES = −2.160), endoplasmic reticulum (NES = − 2.111), ER-golgi intermediate compartment (NES = −2.094), and organelle membrane (NES = −2.094). A full list of gene sets is available in the Supplementary Materials.

## Discussion

In our study, islet synchronization was achieved using a glucose wave (11 ± 1 mM) with a 5-min period. We have used this type of glucose waveform in the past to mimic an in vivo feedback loop that could be used to synchronize islets.[7,12,17] Similar to these previous reports, in the experiments described here, we observed synchronization of islets to the driving frequency when exposed to the glucose wave, and a heterogeneous and asynchronous population was observed when exposed to constant 11 mM glucose. However, we have extended this finding to hypothesize that the vastly different oscillation modes and periodicity between the synchronized and non-synchronized islets, may produce differential gene expression between the two groups. While this design is not an absolute representation of the *in vivo*

environment, the experiment permitted a specific insight into the role of synchronization on gene expression by comparing to the constant glucose treatment. There are other possible mechanisms for *in vivo* synchronization besides glucose oscillations, yet regardless of how they are synchronized, the result would still be a synchronized population of islets with highly homogeneous and periodic oscillations of intracellular metabolites and signals. For this exploratory screen, we elected to utilize microarrays due to their straightforward sample preparation and data analysis workflow.

### Gene sets down-regulated in synchronized islets

GSEA indicated numerous pathways down-regulated in the synchronized population compared to the non-synchronized population. Overall, a general decrease in protein turnover was observed as indicated by down-regulation of the gene sets for protein export, proteasome pathway, endoplasmic reticulum (ER)-related transport, and unfolded protein response (UPR) (Figure 3(a)). This general theme was also observed in the enrichment map (Figure 4) with biosynthesis, ER/respiration, and localization/transport highly ranked clusters. UPR is a process that is induced to alleviate proteotoxic stress due to high levels of protein flux to the ER.[37] Excessive activation of the UPR, and an inability to cope with ER stress, can result in the induction of apoptotic signaling pathways.[38,39] More specific to islets, UPR pathways induced by high glucose have been implicated in beta-cell dysfunction and death.[39] Furthermore, the ER has well-documented $Ca^{2+}$ stores, making it a plausible target for the action of finely-modulated $Ca^{2+}$ oscillations.

More speculatively, the down-regulated gene sets in synchronized islets may suggest a state better adapted to the high glucose environment. Terms related to protein expression and modification (proteasome pathway, translation, metabolism of proteins, and translational initiation) were all down-regulated indicating lower protein turnover. Protein synthesis is one of the most energy-demanding functions in cells[40] so the ability to down regulate these processes could alleviate energy requirements in order to adapt to the high glucose environment. Catabolic processes were also down-regulated in synchronized islets (Figure 4). Typically, catabolic pathways have been found to be activated in times of nutrient stress to fuel and provide building blocks for other cellular processes.[41,42] It may be that that these islets are better adapted to the high glucose environment, resulting in less recycling of metabolic components.

The synchronized population also exhibited down-regulation of the electron transport chain (ETC)-, TCA cycle- and respiration-related gene sets (Figure 3(a)). In addition to these pathways being involved in energy production, the ETC is a primary source of electron leakage and the production of reactive oxidative species (ROS). Islets are known to have low levels of antioxidant enzymes and are susceptible to damage from elevated levels of ROS.[43] As a result, down-regulation of the ETC-related pathways may be beneficial by mitigating ROS production. Several other down-regulated gene sets in the synchronized population may also minimize the production of detrimental byproducts. For example, high protein turnover and UPR-associated pathways were down-regulated (Figure 3 (a)), and both have been affiliated with fibril and plaque formation in islets, resulting in failure and death. Similarly, the formation of glycosaminoglycans has been connected with diabetic pathogenesis and was found to be down-regulated.[44]

Notably, the diabetes pathway gene set was also found to be down-regulated in the synchronized islet population (NES of −2.14 and an FDRq value of 0.0015) (Figures 3(a) and 4). The majority of the genes in the set are associated with binding (47.3%) and catalytic activity (38.2%). Primarily, the down-regulation of this pathway is attributed to the alleviation of $Ca^{2+}$-dependent cytotoxicity. As noted before, this may have been a result of the synchronized population showing more oscillatory behavior compared to the heterogeneous responses in the unsynchronized population.

### Gene sets up-regulated in synchronized islets

Among the gene sets that were up-regulated in synchronized islets were pathways related to the control of cell morphology (Figures 3(b) and 4). For example, gene sets for cell adhesion molecules, extracellular matrix-receptor, and tight-junction interactions were all up-regulated in the synchronized islet

population. The upregulation of these gene sets may be the result of lower $Ca^{2+}$-dependent excitotoxicity in this population, which has been shown to be detrimental to islet morphology and structure.[45-47]

In other cell types, $Ca^{2+}$ oscillations were found to affect the expression of transcription factors and amplify signaling pathways. In our findings, several signaling pathways were also found to be upregulated in the synchronized group, notably, cAMP mediated signaling (Figures 3(b) and 4). This pathway has specifically been shown to be involved in amplification of glucose-induced insulin secretion,[48] potentially leading to an increased response under these conditions.

## Conclusion and future directions

In this report, *in vivo* islet synchronization was mimicked by delivering a low amplitude glucose wave. It was found that a synchronized islet population had a lower drift in oscillation periods due to the forcing of the glucose wave. Additionally, the forcing lowered the number of islets with chronically-elevated $Ca^{2+}$. In turn, these differences in the dynamics may have driven differences in gene expression among these groups, although the exact causative factor is unknown. There are many caveats to this method of *in vitro* synchronization as well as the analysis of gene expression using microarrays. For example, we have not considered many other potential inputs that would occur *in vivo*, it is unknown how islet isolation affects islet behavior or gene expression, and we only examined those genes on the microarray itself. Nevertheless, the system presented here and the resulting dynamics made it easy for this initial comparison of the effects of synchronization on gene expression. Speculatively, the enriched gene sets in the synchronized islets may suggest an efficient adaptation to elevated glucose with lowered amounts of protein turnover, protein translation, and energy production gene sets, which may confer physiological advantages to these islets over a long-term. Much more investigation into this field would be required to confirm this hypothesis.

## Acknowledgments

The authors would like to gratefully acknowledge Mr. Basel Bandak for assistance with islet procurement.

## Disclosure of potential conflicts of interest

No potential conflict of interest was reported by the authors.

## ORCID

Nikita Mukhitov http://orcid.org/0000-0003-4654-3388
Joel E. Adablah http://orcid.org/0000-0003-1628-0281
Michael G. Roper http://orcid.org/0000-0002-0184-1333

## References

1. Henquin JC, Dufrane D, Kerr-Conte J, Nenquin M. Dynamics of glucose-induced insulin secretion in normal human islets. Am J Physiol Endocrinol Metab. 2015;309:E640–E650. doi:10.1152/ajpendo.00251.2015.
2. Boden G, Ruiz J, Urbain JL, Chen X. Evidence for a circadian rhythm of insulin secretion. Am J Physiol. 1996;271:E246–E252. doi:10.1152/ajpendo.1996.271.2.E246.
3. Sturis J, Polonsky KS, Shapiro ET, Blackman JD, O'Meara NM, van Cauter E. Abnormalities in the ultradian oscillations of insulin secretion and glucose levels in type 2 (non-insulin-dependent) diabetic patients. Diabetologia. 1992;35:681–689.
4. Pørksen N, Nyholm B, Veldhuis JD, Butler PC, Schmitz O. In humans at least 75% of insulin secretion arises from punctuated insulin secretory bursts. Am J Physiol. 1997;273:E908–E914.
5. Matveyenko AV, Veldhuis JD, Butler PC. Measurement of pulsatile insulin secretion in the rat: direct sampling from the hepatic portal vein. Am J Physiol Endocrinol Metab. 2008;295:E569–E574. doi:10.1152/ajpendo.90335.2008.
6. Henquin JC. Regulation of insulin secretion: a matter of phase control and amplitude modulaiton. Diabetologia. 2009;52:739–751. doi:10.1007/s00125-009-1314-y.
7. Yi L, Wang X, Dhumpa R, Schrell AM, Mukhitov N, Roper MG. Integrated perfusion and separation systems for entrainment of insulin secretion from islets of Langerhans. Lab Chip. 2015;15:823–832. doi:10.1039/c4lc01360c.
8. Wahren J, Kallas Å. Loss of pulsatile insulin secretion: a factor in the pathogenesis of type 2 diabetes? Diabetes. 2012;61:2228–2229. doi:10.2337/db12-0664.
9. Mao CS, Berman N, Roberts K, Ipp E. Glucose entrainment of high-frequency plasma insulin oscillations in control and type 2 diabetic subjects. Diabetes. 1999;48:714–721.
10. Pedersen MG, Mosekilde E, Polonsky KS, Luciani DS. Complex patters of metabolic and $Ca^{2+}$ entrainment in pancreatic islets by oscillatory glucose. Biophys J. 2013;105:29–39. doi:10.1016/j.bpj.2013.05.036.
11. Lee B, Song T, Lee K, Kim J, Han S, Berggren PO, Ryu SH, Jo J, von Herrath MG. Phase modulation of insulin pulses enhances glucose regulation and enables

inter-islet synchronization. PLoS One. 2017;12: e0172901. doi:10.1371/journal.pone.0172901.
12. Dhumpa R, Truong TM, Wang X, Bertram R, Roper MG. Negative feedback synchronizes islets of Langerhans. Biophys J. 2014;106:2275–2282. doi:10.1016/j.bpj.2014.04.015.
13. Smedler E, Uhlén P. Frequency decoding of calcium oscillations. Biochim Biophys Acta. 2014;1840:964–969. doi:10.1016/j.bbagen.2013.11.015.
14. Dupont G, Goldbeter A. CaM kinase II as frequency decoder of Ca2+ oscillations. Bioessays. 1998;20:607–610. doi:10.1002/(SICI)1521-1878(199808)20:8<607::AID-BIES2>3.0.CO;2-F.
15. Dolmetsch RE, Xu K, Lewis RS. Calcium oscillations increase the efficiency and specificity of gene expression. Nature. 1998;392:933–936. doi:10.1038/31960.
16. Sumit M, Neubig RR, Takayama S, Linderman JJ. Band-pass processing in a GPCR signaling pathway selects for NFAT transcription factor activation. Integr Biol. 2015;7:1378–1386. doi:10.1039/C5IB00181A.
17. Zhang X, Daou A, Truong TM, Bertram R, Roper MG. Synchronization of mouse islets of Langerhans by glucose waveforms. Am J Physiol Endocrinol Metab. 2011;301:E742–E747. doi:10.1152/ajpendo.00248.2011.
18. Dhumpa R, Truong TM, Wang X, Roper MG. Measurement of the entrainment window of islets of Langerhans by microfluidic delivery of a chirped glucose waveform. Integr Biol. 2015;7:1061–1067. doi:10.1039/C5IB00156K.
19. Subramanian A, Tamayo P, Mootha VK, Mukherjee S, Ebert BL, Gillette MA, Paulovich A, Pomeroy SL, Golub TR, Lander ES, et al. Gene set enrichment analysis: a knowledge-based approach for interpreting genome-wide expression profiles. Proc Natl Acad Sci USA. 2005;102:15545–15550. doi:10.1073/pnas.0506580102.
20. Subramanian A, Kuehn H, Gould J, Tamayo P, Mesirov JP. GSEA-P: a desktop application for gene set enrichment analysis. Bioinformatics. 2007;23:3251–3253. doi:10.1093/bioinformatics/btm369.
21. Xia Y, Whitesides GM. Soft lithography. Annu Rev Mater Sci. 1998;28:153–184. doi:10.1146/annurev.matsci.28.1.153.
22. Irizarry RA, Hobbs B, Collin F, Beazer-Barclay YD, Antonellis KJ, Scherf U, Speed TP. Exploration, normalization, and summaries of high density oligonucleotide array probe level data. Biostatistics. 2003;4:249–264. doi:10.1093/biostatistics/4.2.249.
23. Gautier L, Cope L, Bolstad BM, Irizarry RA. affy–analysis of Affymetrix genechip data at the probe level. Bioinformatics. 2004;20:307–315. doi:10.1093/bioinformatics/btg405.
24. Gentleman RC, Carey VJ, Bates DM, Bolstad B, Dettling M, Dudoit S, Ellis B, Gautier L, Ge Y, Gentry J, et al. Bioconductor: open software development for computational biology and bioinformatics. Genome Biol. 2004;5:R80. doi:10.1186/gb-2004-5-10-r80.
25. Dai M, Wang P, Boyd AD, Kostov G, Athey B, Jones EG, Bunney WE, Myers RM, Speed TP, Akil H, et al. Evolving gene/transcript definitions significantly alter the interpretation of genechip data. Nucleic Acids Res. 2005;33:e175. doi:10.1093/nar/gni179.
26. Brettschneider J, Collin F, Bolstad BM, Speed TP. Quality assessment for short oligonucleotide microarray data. Technometrics. 2008;50:241. doi:10.1198/004017008000000334.
27. Benjamini Y, Hochberg Y. Controlling the false discovery rate: a practical and powerful approach to multiple testing. J Roy Statist Soc Ser B. 1995;57:289–300.
28. NCBI Resource Coordinators. Database resources of the national center for biotechnology information. Nucleic Acids Res. 2013;41:D8–D20. doi:10.1093/nar/gks1189.
29. Merico D, Isserlin R, Stueker O, Emili A, Bader GD. Enrichment map: a network-based method for gene-set enrichment visualization and interpretation. PLoS One. 2010;5:e13984. doi:10.1371/journal.pone.0013984.
30. Nunemaker CS, Zhang M, Wasserman DH, McGuinness OP, Powers AC, Bertram R, Sherman A, Satin LS. Individual mice can be distinguished by the period of their islet calcium oscillations: is there an intrinsic islet period that is imprinted in vivo? Diabetes. 2005;54:3517–3522.
31. Bertram R, Satin L, Zhang M, Smolen P, Sherman A. Calcium and glycolysis mediate multiple bursting modes in pancreatic islets. Biophys J. 2004;87:3074–3087. doi:10.1529/biophysj.104.049262.
32. Yi L, Bandak B, Wang X, Bertram R, Roper MG. Dual detection system for simultaneous measurement of intracellular fluorescent markers and cellular secretion. Anal Chem. 2016;88:10368–10373. doi:10.1021/acs.analchem.6b02404.
33. Schrell AM, Mukhitov N, Yi L, Adablah JE, Menezes J, Roper MG. Online fluorescence anisotropy immunoassay for monitoring insulin secretion from islets of Langerhans. Anal Methods. 2017;9:38–45. doi:10.1039/C6AY02899C.
34. He K, Lv W, Zhang Q, Wang Y, Tao L, Liu D. Gene set enrichment analysis of pathways and transcription factors associated with diabetic retinopathy using a microarray dataset. Int J Mol Med. 2015;36:103–112. doi:10.3892/ijmm.2015.2220.
35. Taneera J, Storm P, Groop L. Downregulation of type II diabetes mellitus and maturity onset diabetes of young pathways in human pancreatic islets from hyperglycemic donors. J Diabetes Res. 2014;2014:237535. doi:10.1155/2014/237535.
36. Kim S, Kon M, Delisi C. Pathway-based classification of cancer subtypes. Biol Direct. 2012;7:21. doi:10.1186/1745-6150-7-21.

37. Reid DW, Chen Q, Tay AS, Shenolikar S, Nicchitta CV. The unfolded protein response triggers selective mRNA release from the endoplasmic reticulum. Cell. 2014;158:1362–1374. doi:10.1016/j.cell.2014.08.012.
38. Back SH, Kaufman RJ. Endoplasmic reticulum stress and type 2 diabetes. Annu Rev Biochem. 2012;81:767–793. doi:10.1146/annurev-biochem-072909-095555.
39. Lee JH, Won SM, Suh J, Son SJ, Moon GJ, Park UJ, Gwag BJ. Induction of the unfolded protein response and cell death pathway in Alzheimer's disease, but not in aged Tg2576 mice. Exp Mol Med. 2010;42:386–394. doi:10.3858/emm.2010.42.5.040.
40. Pereira SF, Gonzalez RL Jr., Dworkin J. Protein synthesis during cellular quiescence is inhibited by phosphorylation of a translational elongation factor. Proc Natl Acad Sci USA. 2015;112:E3274–E3281. doi:10.1073/pnas.1505297112.
41. Boroughs LK, DeBerardinis RJ. Metabolic pathways promoting cancer cell survival and growth. Nat Cell Biol. 2015;17:351–359. doi:10.1038/ncb3124.
42. Yuan HX, Xiong Y, Guan KL. Nutrient sensing, metabolism, and cell growth control. Mol Cell. 2013;49:379–387. doi:10.1016/j.molcel.2013.01.019.
43. Robertson RP, Harmon JS. Pancreatic islet β-cell and oxidative stress: the importance of glutathione peroxidase. FEBS Lett. 2007;581:3743–3748. doi:10.1016/j.febslet.2007.03.087.
44. Gowd V, Gurukar A, Chilkunda ND. Glycosaminoglycan remodeling during diabetes and the role of dietary factors in the modulation. World J Diabetes. 2016;7:67–73. doi:10.4239/wjd.v7.i4.67.
45. Stancill JS, Cartailler JP, Clayton HW, O'Connor JT, Dickerson MT, Dadi PK, Osipovich AB, Jacobson DA, Magnuson MA. Chronic β-cell depolarization impairs β-cell identity by disrupting a network of $Ca^{2+}$-regulated genes. Diabetes. 2017;66:2175–2187. doi:10.2337/db16-1355.
46. Clark AL, Kanekura K, Lavagnino Z, Spears LD, Abreu D, Mahadevan J, Yagi T, Semenkovich CF, Piston DW, Urano F. Targeting cellular calcium homeostasis to prevent cytokine-mediated beta cell death. Sci Rep. 2017;7:5611. doi:10.1038/s41598-017-05935-4.
47. Giannone G, Rondé P, Gaire M, Beaudouin J, Haiech J, Ellenberg J, Takeda K. Calcium rises locally trigger focal adhesion disassembly and enhance residency of focal adhesion kinase at focal adhesions. J Biol Chem. 2004;279:28715–28723. doi:10.1074/jbc.M404054200.
48. Howell SL, Jones PM, Persaud SJ. Regulation of insulin secretion: the role of second messengers. Diabetologia. 1994;37:S30–S35.